Journal Pre-proofs

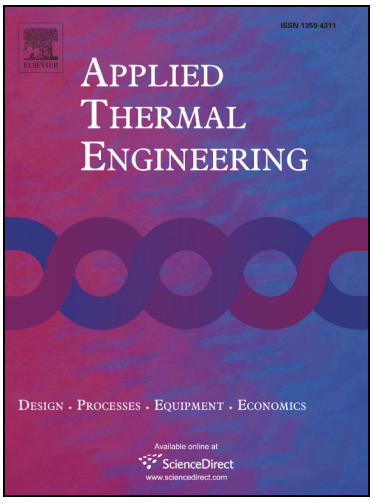

Toward one-hundred-watt-level applications of quantum dot converters in high-power light-emitting diode system using water-cooling remote structure

Zong-Tao Li, Yong-Jun Chen, Jia-Sheng Li, Shun-Ming Liang, Yong Tang

PII: S1359-4311(20)33148-3
DOI: https://doi.org/10.1016/j.applthermaleng.2020.115666
Reference: ATE 115666

To appear in: *Applied Thermal Engineering*

Received Date: 16 January 2020
Revised Date: 20 June 2020
Accepted Date: 24 June 2020

Please cite this article as: Z-T. Li, Y-J. Chen, J-S. Li, S-M. Liang, Y. Tang, Toward one-hundred-watt-level applications of quantum dot converters in high-power light-emitting diode system using water-cooling remote structure, *Applied Thermal Engineering* (2020), doi: https://doi.org/10.1016/j.applthermaleng.2020.115666

Toward one-hundred-watt-level applications of quantum dot converters in high-power light-emitting diode system using water-cooling remote structure

Zong-Tao Li[1, 2], Yong-Jun Chen[1], Jia-Sheng Li[1, 2,*], Shun-Ming Liang[1], and Yong Tang[1]

[1]National & Local Joint Engineering Research Center of Semiconductor Display and Optical Communication Devices, South China University of Technology, Guangzhou 510641, China
[2]Foshan Nationstar Optoelectronics Company, Ltd., Foshan 528000, China
[*]Correspondence: jiasli@foxmail.com;

Abstract

Quantum dots (QDs) face severe heat dissipation challenges when packaged with high-power light-emitting diodes (HPLEDs). In this study, a water-cooling remote (wc-remote) structure was proposed to significantly improve the heat dissipation of QD converters in a HPLED system. The QD converter was removed from the HPLED sources to isolate the thermal power generated from the chips and was assembled on a transparent glass chamber filled with flowing water for heat dissipation. The thermal performances and optical stability of the QD converters were investigated with different device structures, electrical injection powers, and flow rates. The results demonstrate that the optimized wc-remote structure reduced the maximum steady temperature of the QD converters to 71 °C at an ultrahigh electrical injection power of 100 W, while those for the conventional on-chip and remote structures were reduced by 453 and 265 °C, respectively. Operating aging tests confirmed that the wc-remote structure exhibits a slow degradation and almost no redshift in the optical spectra, contributing to a lifetime of 2~3 orders of magnitude longer than that of conventional structures. The proposed wc-remote structure can be a respectable start point for QD converters in hundred-watt-level applications, such as projection illumination and display.

Keywords: High-power light-emitting diodes; quantum dot color converter; water cooling; operating temperature; lifetime.

1 Introduction

Light emitting diodes (LEDs) have been widely used in many fields, including street lamps, advertising displays, automotive headlights, and traffic lights[1, 2]. The wide application of LEDs can be attributed to their advantages of energy-saving, long service time, small dimension, and low-cost[3, 4]. At present, most color converters in LEDs are based on yttrium aluminum garnet (YAG) phosphor with high thermal stability[5, 6]. Compared with YAG phosphor, there are many advantages of quantum dots (QDs) as color converters in LEDs, including a narrow full width at half maximum (FWHM), high photoluminescent quantum yield (PLQY), and tunable emission wavelength[7-9]. A wider color gamut[10, 11]and higher color rendering index[12, 13]have been successfully achieved for display and illumination applications, respectively, using state-of-the-art

QD converters. However, QD converters continue to encounter stability challenges in LEDs owing to their natural thermal instability[14]. According to previous studies, it can easily lead to fluorescence quenching of QDs when the operating temperature is over 80 ℃[15]. Moreover, the dispersing matrix (like silicone) can become carbonized when the operating temperature reaches about 350 ℃[16]. Generally, the high operating temperature of QD converters is attributed to the large conversion loss (≥60%) at high QD concentration (for white light generation) responsibly by the aggregation and reabsorption loss[17]. Thus, a large portion of the light from LED chips absorbed by QD converters transforms into thermal power by the nonradiative recombination[18]. Moreover, the low thermal conductivity of a QD dispersing matrix (e.g., silicone) suppresses the heat dissipation of QDs[19]. Therefore, QD-LEDs can only maintain a relatively stable light output at an injection electrical power lower than ~0.1 W[20] to minimize the thermal impact.

Great efforts have been put into improving the thermal performance of QD-LEDs, such as incorporating nanoparticles with high thermal conductivity to increase the heat dissipation of the polymer matrix[21, 22]. However, this improvement is limited by the low incorporating concentration considering the optical loss introduced by nanoparticles. To maintain high optical efficiency, the heat dissipation can also be strengthened to a certain extent by shortening the heat path from QDs to the LED chip and substrate, which can be treated as a heat sink for QDs[23]. Most of these studies are focused on low-power LEDs with milliwatt-level injection electrical power, the thermal influence of an LED chip on QDs is generally negligible. When the injection electrical power is increased over watt level, the fast degradation of QD converters can be observed after operating within seconds owing to the serious heat power generation from the chips[24]. Therefore, the removal of the QD converter away from the LED chips is highly recommended by inserting air for thermal isolation[25], which is known as a remote structure. The operating temperature of color converters can be further reduced by combining with graphene[26] or a sapphire plate[27] with high thermal conductivity, while the heat dissipation remains limited owing to the inefficient natural convection. Our previous work demonstrated that the operating temperature of color converters can be largely reduced by ~400 °C using a heat pipe substrate, the excitation source is an external laser with the optical power of 32 W[16]. However, one major concern is that the substrate for QD converters in a HPLED system should have high transmittance to ensure the efficient optical output, most thermal management techniques for LED chips, including microchannels[28], thermoelectric[29, 30], and heat pipe[31-33], are with poor light transmittance and difficult to adopt for QD converters. In this study, a water cooling-remote (wc-remote) method was developed to reduce the operating temperature and increase the lifetime of QD-HPLEDs. First, the thermal performances of QD-HPLEDs with different structures were investigated in detail with various injection electrical powers and the optimum flow rate was determined. Then, the stabilities of their optical spectra were further compared to study the thermal effect on the color conversion processes. Finally, aging tests at a continuous injection current of 100 W were performed to confirm the high thermal performances and optical stability of the proposed wc-remote structure.

2 Experiments

The QD-HPLEDs used in this study comprised a HPLED source, QD converter, and heat sink. The HPLED source was packaged by a chip-on-board structure with 100 pieces of blue GaN-based LED chips[34] and a silicone encapsulant. The QD converter was fabricated by blade coating. In detail, CdSe-based QDs (centered wavelength of 525±2 nm, PLQY ≥ 80%, FWHM ≤ 30 nm) were

dispersed in a silicone matrix by mechanical stirring with solvent evaporation[11]. Then, the thickness of the QD-silicone mixture was controlled by blade coating and finally the mixture was cured in an oven with a temperature of 90 °C for 45 min. The QD converter had a thickness of 0.5 mm and a mass concentration of 1.5 wt.%. The heat sink used in all cases was an aluminum-based fin with a 1.5 W fan. The on-chip structure can use the substrate including LED chips as a heat dissipating element at low power, while the remote structure can avoid the thermal impact of LED chips at high power. Therefore, these two structures are most widely used in QD-LEDs. As shown in Figs. 1(a) and (b), four kinds of device structures were investigated. The QD converter was directly assembled on the HPLED source to obtain the on-chip structure generally applied at milliwatt-level injection power[35], while it was assembled away from the HPLED at a distance of 55 mm to obtain the remote structure generally applied at watt-level injection power. [36]. In this study, the combination of water-cooling and remote structure is used for QD-LEDs with a higher injection power. Regarding the proposed wc-remote structure, a transparent water-filled silica glass chamber (SGC) was introduced to the remote QD converter, which was fabricated by high-temperature melt welding. The thermal conductivity of silica glass is 1.09 W/(m·K). Unbaffled and baffled SGCs were investigated; their structural parameters are summarized in Table 1. Moreover, the experimental setups are shown in Fig. 1(c). The circulating cooling water in SGC was driven by a peristaltic pump (Kamoer, CK15) for continuous and stable water flow (water bath temperature of 25 °C) and the accuracy of the flow rate is ±1 %. The inlet and outlet connectors are realized by connecting the glass tube of the SGC with a silica gel tube. The transient temperature and steady temperature field were measured by infrared cameras (A655SC, FLIR SYSTEMSAB, Seattle, WA, USA) mounted on a tripod and the accuracy of the measured temperature is ±2 ℃. The distance between the camera lens and QD convertors is 0.4 m. In addition, we used an opaque black cloth to block the infrared camera and the QD-LED to avoid the impact of environmental infrared radiation. The injection electrical power of the HPLED sources ranged from 20 to 100 W was provided by a DC source. The optical spectra were measured by an integrating sphere system as shown in Fig. 1(d). We put the QD-HPLED into the integrating sphere with a diameter of 1.2 m and connected the integrating sphere with the computer through a spectrometer (Ocean Optics USB2000+). In addition, the QD-HPLED is connected with the rubber tube of a peristaltic pump through a small hole of the integrating sphere. The ambient temperature for the thermal and optical measurements was 25 °C.

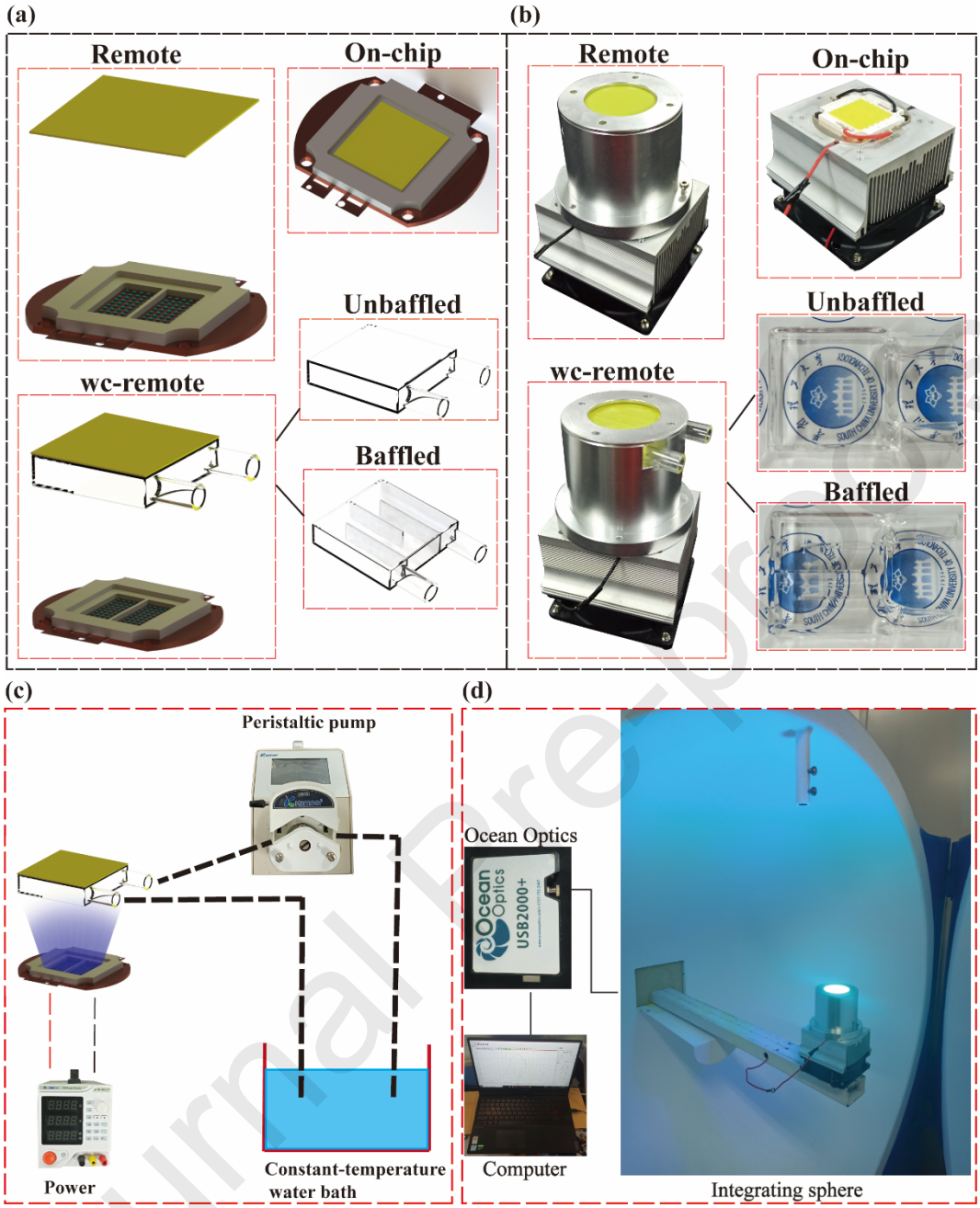

Fig. 1. (a) Schematic diagram and (b) photographs of the four kinds of device structures. (c) Schematic of the experimental setup. (d) Photographs of the QD-LED device in the integrating sphere system.

Table 1 Structural parameters of the glass plate.

Parameter	Baffled SGC	Unbaffled SGC
Size	40 mm(L) × 40 mm(W) × 10 mm(H)	40 mm(L) × 40 mm(W) × 10 mm(H)
Flow path width	8.75 mm	No flow paths
Flow path height	8 mm	No flow paths
Baffle length	30 mm	No baffle
Baffle number	3	No baffle
Working fluid	Water	Water

Glass thickness	1 mm	1 mm

3. Results and discussion

3.1. Thermal performance

The thermal performance of the QD-HPLEDs was compared using four device structures, as illustrated above. All these devices were measured at an injection electrical power of 100 W and the flow rate for the wc-remote structure was maintained at 7 mL/min. The emissivity of silicone gel is set as 0.96[37, 38]. In addition, the precise temperature measurement of phosphor particles in the color conversion layer has always been a difficult academic problem. In this article, we use the surface temperature of the whole film for comparative analysis, which is the same as most previous studies[20-22, 27, 39]. The transient temperature of QD converters at the surface hotspot for different HPLEDs is shown in Fig. 2(a). It is seen that the transient temperature of the on-chip structure, remote structure, unbaffled wc-remote structure, and baffled wc-remote structure reached 524, 336, 132, and 126 °C, respectively, as the operating time increased and then steadied. Notably, carbonization occurred in the QD converter within seconds when using the on-chip structure[24], as shown in Fig. 2(b). Therefore, the transient temperature was recorded just before carbonization. For convenience, the transient temperature at the time carbonization occurred is approximately considered as the steady temperature for subsequent comparisons. At an injection electrical power of 100 W, the temperature of QD convertors in the on-chip structure can reach up to 524 °C. However, the average temperature of the top surface of the substrate is only about 35 ℃. It can be inferred that the maximum junction temperature of LED chips is less than 85 ℃ according to the basic thermal resistance model[40]. Generally, GaN-based blue LED chips can operate normally[41] below a junction temperature of 90 ℃.

In addition, the HPLED source also served as the heat sink for the QD converter owing to its more effective heat dissipation compared with the natural convection by air[42]. Previous studies on low-power LEDs have indicated that the on-chip structure is more beneficial for QD heat dissipation. It is because that the QD convertor in the on-chip structure closer to the heat sink (LED chip or substrate) has a better heat dissipation ability compared with the remote structure[25]. In our cases, the steady temperature of the on-chip structure is 188 °C higher than that of the remote structure. These results are mainly because the LED chips also serve as a heat source for the QD converter because their external quantum efficiency is always less than unity. Regarding solving this issue, Fig. 2(c) shows the transient temperature of the HPLEDs without the integration of QD converters. The steady temperature reaches as high as 74 °C, though such temperature is safe for LED chips while it suppresses the heat dissipation of the QD converter to the heat sink at the bottom due to the poor thermal conductivity of silicone matrix. The faster heating rate of the remote structure shown in Fig. 2(a) can further support this explanation. In addition, the hotspot is located in the central region of the QD converters owing to the Lambert lighting distribution of the LEDs, which can be observed by the steady temperature field shown in Fig. 2(d). The on-chip structure has a higher irradiance on the QD converter compared with the remote structure owing to the lesser amount of free space for light divergence. Thus, the center (hotspot) of the QD converter in the on-chip structure can absorb much more high-power-density blue light and leads to a higher steady temperature compared with the remote structure. As a result, the remote structure is highly

recommended in HPLEDs considering all these factors. However, a limitation remains in the remote structure that the heat dissipation is generally based on natural convection, resulting in a high steady temperature of 336 °C. This limitation can be easily overcome by introduction of a SGC. The steady temperature of the unbaffled wc-remote structure is just 132 °C, which decreases by 204 °C compared with the conventional remote structure. Moreover, the baffled wc-remote structure has a lower steady temperature (decreased by 6 °C) and a more uniform temperature field compared with the unbaffled wc-remote structure, as shown in Fig. 2(d). These results come from the fact that the baffle can avoid the short-circuit of fresh fluid from inlet to outlet, and the channels increase the contact area between silica glass and water, which contributes to an enhanced heat transfer[43].

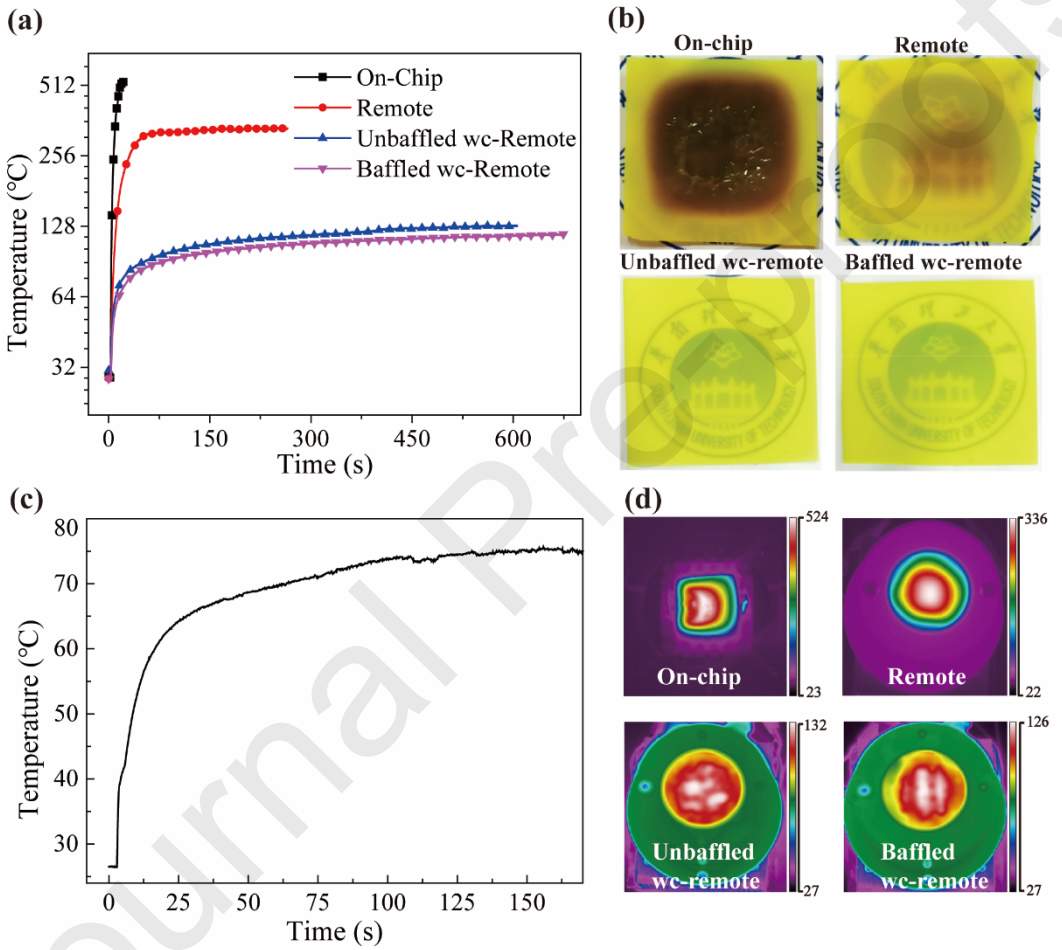

Fig. 2. Thermal performance comparisons using on-chip, remote, unbaffled wc-remote, and baffled wc-remote structures. (a)The transient temperature of QD-HPLEDs. (b) Photographs of QD converters in different device structures after operating at 100 W for 20 s. (c) The transient temperature of blue HPLEDs without QD converters. (d) Steady temperature field, the unit is °C.

Moreover, the initial optical spectra of the different remote structures were compared to evaluate the effect of the SGC on the light output, as shown in Fig. 3(a). The thermal effect can be ignored in this case with an injection electrical power as low as 1 W. It is evident that the spectra exhibit almost no changes after integrating with the baffled or unbaffled SGC. The transmittance spectra were obtained to investigate this issue, as shown in Fig. 3(b). Here, it can be seen that the baffled and unbaffled SGCs both have a high diffuse transmittance (approximately 90%) from 300 nm to

800 nm, which are only slightly lower than that of the referenced PDMS film. Therefore, the SGC also ensures high optical efficiency for HPLED systems. Considering both the thermal and optical performances, we only focused on the baffled SGC in the wc-remote structure when studying the injection electrical power and flow rate at subsequence.

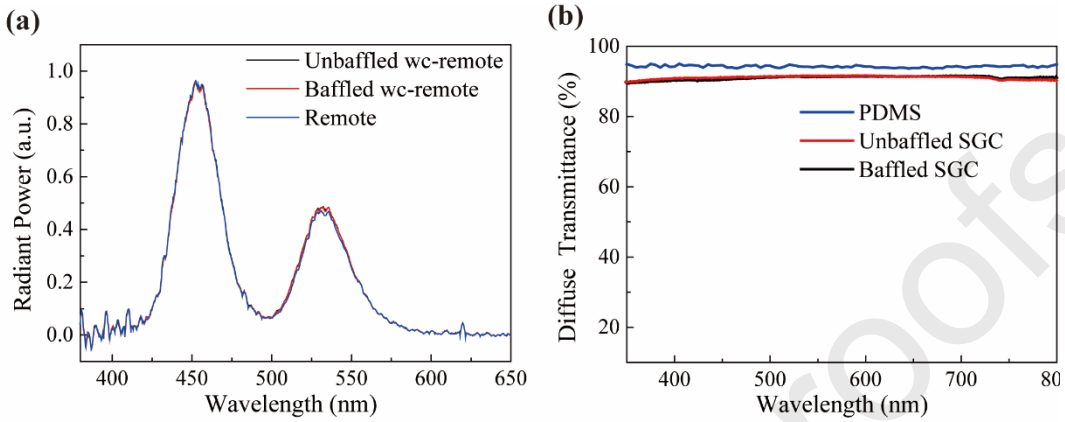

Fig. 3. (a) Initial optical spectra of different remote structures under an injection electrical power of 1 W. (b) Diffuse transmittance of blank PDMS (0.5 mm), baffled SGC, and unbaffled SGC.

To investigate the effect of the flow rate on the wc-remote structure, the flow rate values were set as 0–120 mL/min under different injection electrical powers. All these temperatures were measured using an infrared camera, which only characterizes the surface temperature of devices. The transient temperatures of the wc-remote QD converters at the surface hotspots under 20, 40, 70, and 100 W injection electrical powers are given in Figs. 4(a)–(d), respectively. The transient temperature continues to increase for QD converters with 0 mL/min (the SGC is filled with water and then sealed) and has difficulty reaching a steady state even after 5 min owing to the high heat capacity of water. When heat transfer occurs in the SGC by water flowing, less time is required to reach a steady temperature and the steady temperature becomes lower with an increasing flow rate. These results are mainly because the heat generated from the QD converter can be removed faster when the flow rate increases. To further support this, Figs. 5(a) and (b) show the steady temperature field of the wc-remote QD converters with flow rates of 7 and 120 mL/min, respectively. The steady temperature and the hotspot area of the QD converter with a flow rate of 120 mL/min are significantly smaller than that with 7 mL/min. In addition, the on-chip and remote structures are set as the reference structures for comparisons, their transient temperatures are shown in Fig. 4. Notably, the QD converters in the on-chip structure with an injection electrical power larger than 70 W start carbonization within just a few seconds. As discussed above, we only focused on the thermal power generated from the QDs, thereby the transient temperature at the start point of carbonization is approximately treated as the steady temperature for the on-chip structure to neglect the effect of the subsequent carbonization process on the thermal power. Similarly, the steady temperature field of these on-chip and remote structures are given in Figs. 5(c) and (d), respectively. It is clear that a large temperature difference between the QD converter and the holder was observed as the injection electrical power increased for both the on-chip and remote structures. However, a smaller temperature difference (i.e., a more uniform temperature distribution) was observed for the wc-remote structures with increasing injection electrical power, as shown in Figs. 5(a) and (b), the

temperature of the holder became increasingly larger than the environmental temperature. These results demonstrate that the heat difficultly transfers from the QD converter to the holder in the on-chip and remote structures owing to the low thermal conductivity of the silicone matrix (0.3 W/(m·K)[25]) and the inefficient natural convection. However, the SGC with higher thermal conductivity (silica glass-1.09 W/(m·K)[44],water-0.61 W/(m·K)[45]) successfully enhanced the heat transfer performance of the whole system, avoiding the thermal power concentrated within the QD converter in the wc-remote structure.

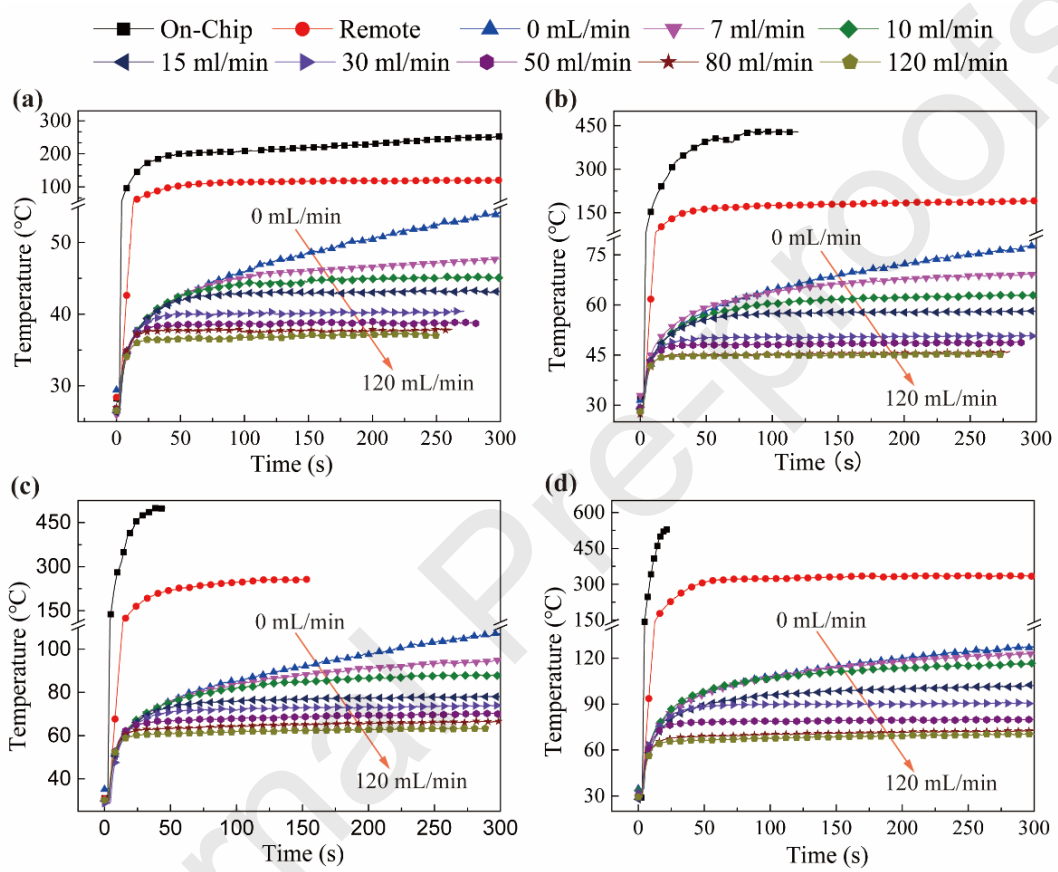

Fig. 4. Transient temperatures of color converters in the wc-remote structure with different flow rates. (a)–(d) Injection electrical powers of 20, 40, 70, and 100 W, respectively. The on-chip and remote structures are set as references.

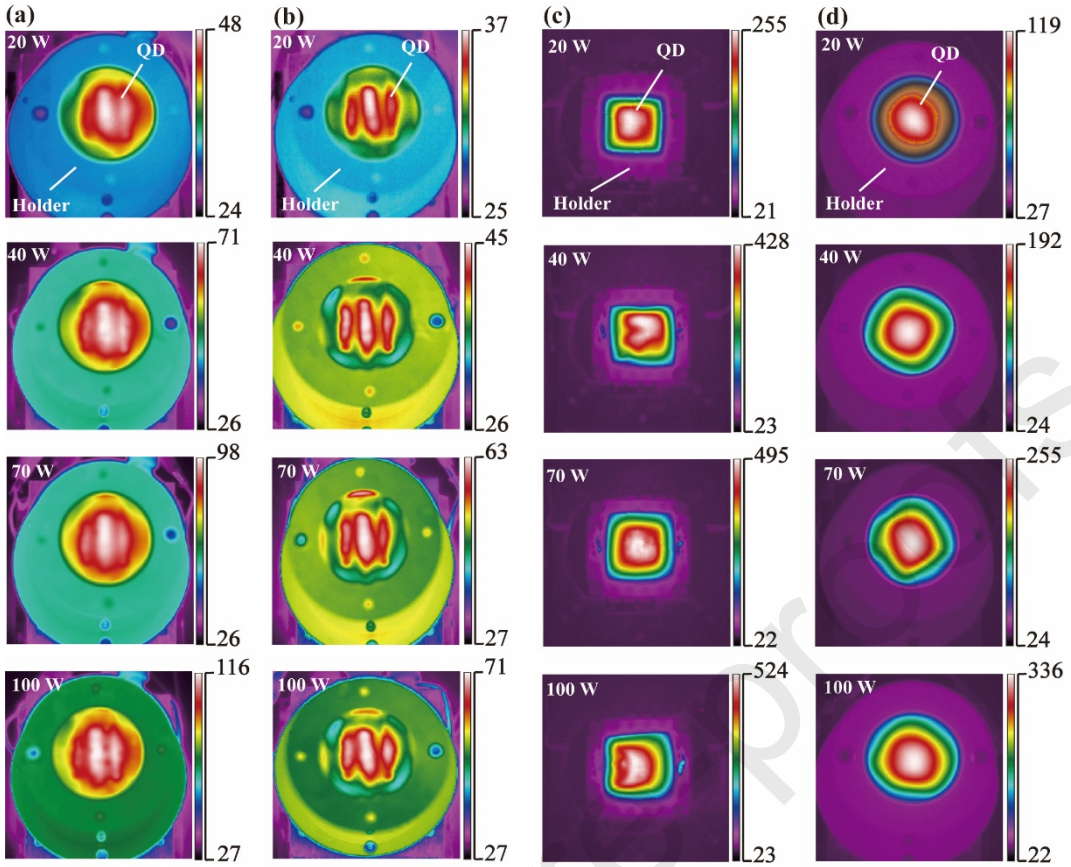

Fig. 5. Steady temperature fields of QD-HPLEDs with different injection electrical powers, the unit is °C. (a) wc-remote structure with flow rate of 7 mL/min; (b) wc-remote structure with flow rate of 120 mL/min; (c) On-chip structure; (d) Remote structure.

The maximum steady temperature of the QD converters in the wc-remote structure with different flow rates and injection electrical powers is further summarized in Fig. 6(a). As the flow rate increases, the maximum steady temperature reduces and gradually tends to be constant at a saturated flow rate. This is because the temperature difference between the water and SGC becomes larger when the flow rate increases, which contributes to better heat dissipation. When the flow rate reaches saturation, the temperature of the water in the SGC tends to be the same with a constant water bath temperature. Therefore, the temperature difference between the water and SGC tends to remain constant, which leads to the almost-constant maximum steady temperature, even though the flow rate exceeds the saturated flow rate. Moreover, a larger saturated flow rate is required when using higher injection electrical power. This is because the temperature of the QD converter will be higher with an increased injection electrical power, which leads to more heat transfer to the water. A larger saturated flow rate is required for the water temperature in the SGC to become close to the constant water bath temperature. In our cases, the maximum steady temperature had almost no change at a high injection electrical power of 100 W when the flow rate reached 120 mL/min, the maximum steady temperature reduced by 44% compared with that using a flow rate of 7 mL/min. As a result, 120 mL/min was selected as the optimum flow rate at subsequence. Fig. 6(b) shows the maximum steady temperature of the QD converters in the on-chip and remote structures for comparisons. As the injection electrical power increased from 20 to 100 W, the maximum steady temperature for the on-chip and remote structures increased from 255 to 524 °C and 119 to 336 °C,

respectively, which is hardly acceptable in practice. However, the wc-remote structure can significantly reduce the maximum steady temperature of the QD converter at each corresponding injection electrical power compared with the reference structures. The comparison results are summarized in Table 2 for convenience. Although an ultrahigh injection electrical power of 100 W was used, the maximum steady temperature in the wc-remote structure reduced to 71 °C, which is 453 °C (reduced by 86.5%) and 265 °C (reduced by 78.9%) lower than those of the on-chip and remote structures, respectively. These results demonstrate that the wc-remote structure is essential for QD converters to reduce the operating temperature at hundred-watt-level applications.

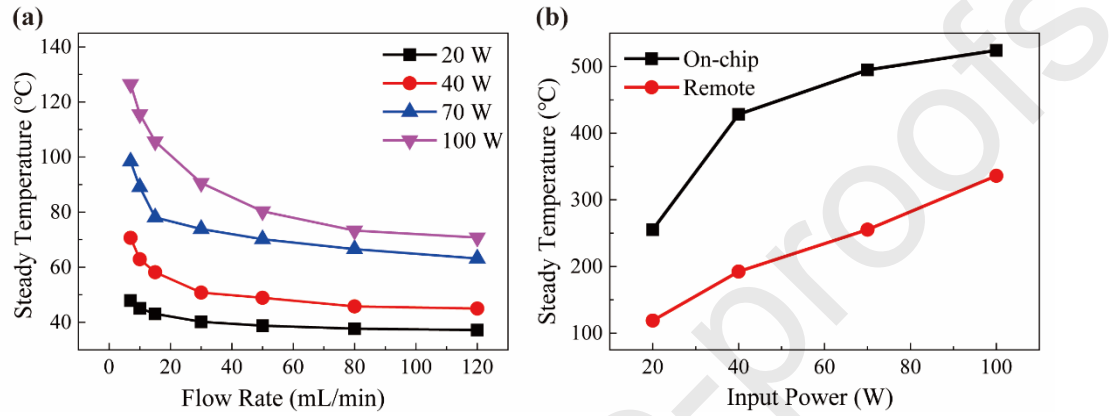

Fig. 6. (a) Maximum steady temperature of QD-HPLEDs with the wc-remote structure under different flow rates and injection electrical powers. (b) Maximum steady temperatures of QD-HPLEDs with traditional on-chip and remote structures under different injection electrical powers.

Table 2 Comparison results of wc-remote structure and on-chip structure/remote structure.

Injection electrical power (W)	Maximum steady temperature (°C)		
	wc-remote structure	remote structure	on-chip structure
20	37	82	218
40	45	147	383
70	63	192	432
100	71	265	453

The infrared camera can only measure the surface temperature of QD convertors; therefore, the fluid (water) temperature is analyzed by the fluid and thermal coupling simulation. Herein, we used the cases with an injection electrical power of 100 W as examples. The temperature distributions of the SGC were simulated by the coupling of fluid flow module and steady-state thermal module in ANSYS software. The critical parameters used for simulation are listed in Table 3. The QD convertor was set as a heat source and the heat power was 17.6 W, which was calculated according to the previous study[18].

The simulated fluid temperature distributions of the wc-remote structure are given in Fig. 7. It is seen that the average temperature difference between the inlet and outlet is 24.9 ℃ and 2.1 ℃ with a flow rate of 7 and 120 ml/min, respectively. We can see that the fluid temperature at a lower region with the flow rate of 7ml/min is much higher than that with the flow rate of 120 ml/min. Moreover, the fluid temperature at the lower region is about the same as the fluid temperature at the inlet when the flow rate is 120 ml/min, and the average temperature difference between the inlet and outlet is

2.1 °C. These results indicate that the heat transfer performance of the SGC has been basically reached to the maximum at this flow rate. In the future, the structural parameters of the SGC can be optimized to further improve the heat dissipation performance of QD convertors.

In addition, thermal resistance is an important property for evaluating the heat dissipation performance of LED devices. The temperature fields of QD convertors integrated on the SGC (wc-remote structure) with the flow rate of 7 and 120 ml/min are given in Fig. 8(a) and (b), respectively. The temperature field of a traditional QD convertor (remote structure) is shown in Fig. 8 (c). Notably, the simulated temperature error is ~5% compared with the experiment results, which probably depends on the accuracy of the thermal conductivity, geometry and convection coefficient. In this case, the thermal resistance from the QD convertor to the bottom of the SGC (R_{qd-btm}) for the wc-remote structure is evaluated by the following equation:

$$R_{qd-btm} = (T_{qd} - T_{btm})/P_{qd}, \quad (1)$$

Here, P_{qd} is the heat power of a QD convertor, T_{qd} is the average temperature of a QD convertor, and T_{btm} is the average temperature of the bottom surface of a SGC. According to simulations, the R_{qd-btm} of the wc-remote structure is 4.39 and 1.97 K/W with a flow rate of 7 and 120 ml/min, respectively, which can be reduced by 55.1% after the flow rate is optimized. According to the simulated temperature of the inlet and outlet, the thermal power extracted by the liquid loop (Q_W) can be easily obtained as 732.1 and 1058.4 J/min with a flow rate of 7 and 120 ml/min, respectively, which can be also increased by 44.6% after the flow rate is optimized. As for the conventional remote structure, its thermal resistance is as high as 18.7 K/W. Therefore, the thermal resistance of the optimal wc-remote structure can be reduced by 89.5% compared with the traditional remote structure. These results well suggest the importance of the wc-remote structure for improving the heat dissipation of QD convertors.

Table 3 Critical parameters used for simulation.

Parameters	QD convertor	Silica glass	Water
Thermal conductivity (W/(m·K))	0.3	1.09	0.59
Specific heat capacity (cal/(g·K))	0.2	0.213	0.999
Thickness (mm)	0.5	/	/
Inlet temperature (°C)	/	/	25

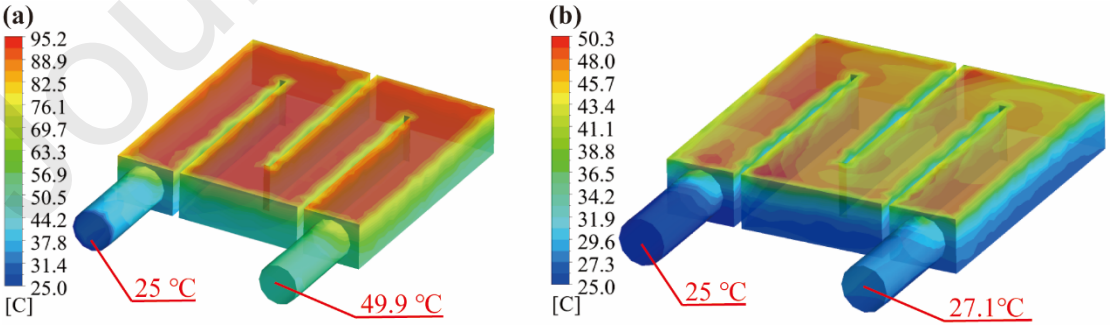

Fig. 7. Simulated fluid temperature fields in SGC of the wc-remote structure with the flow rate of (a) 7 ml/min and (b) 120 ml/min. The injection electrical power of LEDs is 100 W.

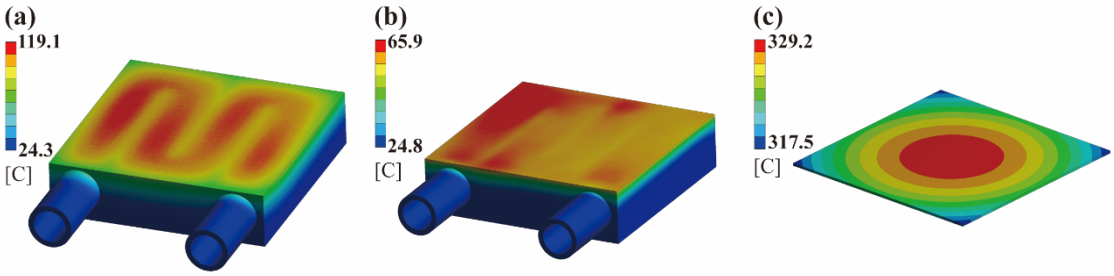

Fig. 8. Simulated temperature fields of wc-remote structures with the flow rate of (a) 7 ml/min and (b) 120 ml/min. (c) Simulated temperature fields of a conventional remote structure. The injection electrical power of LEDs is 100 W.

3.2. Optical Stability

The optical stability of the QD-HPLEDs was obtained to further confirm the excellent thermal performance using the wc-remote structure. For this section, the wc-remote structure had an optimized flow rate of 120 mL/min, as discussed above. Figs. 9 (a)–(c) show the electroluminescence (EL) spectra stability using the on-chip, remote, and wc-remote structures, respectively. The blue peak (380–490 nm) and green peak (490–600 nm) originates from the LED chips and QD converters, respectively. In Fig. 9(a), the green peak intensity of the on-chip structure decreases quickly, within seconds, even at a relatively low injection electrical power of 20 W, and the decrement of the green peak intensity from 0 to 10 min is 71.4%, which is attributed to the high operating temperature of the QD converter as in Fig. 6(b). When the injection electrical power is 100 W, it takes only 30 s for the green peak intensity to reduce by 91.1%. Meanwhile, the green peak intensity of the remote structure shown in Fig. 9(b) reduces more slowly than that of the on-chip structure. However, a fast degradation was still observed at the high injection electrical power of 100 W, the green peak intensity decreased by 70.5% after operating for 6 min. It should be noted that the blue peak intensity of these two structures also reduces owing to the silicone carbonization that increases the blue light absorption. Furthermore, the blue peak intensity of the wc-remote structure shown in Fig. 9(c) hardly decreases, even at an injection electrical power of 100 W, and the green peak intensity only decreases by 25.4% after operating for 10 min. In addition, a redshift of the green peak of the on-chip and remote structures clearly appears as the operating time increases, particularly at a larger injection electrical power, while the green peak of the wc-remote structure has almost no redshift.

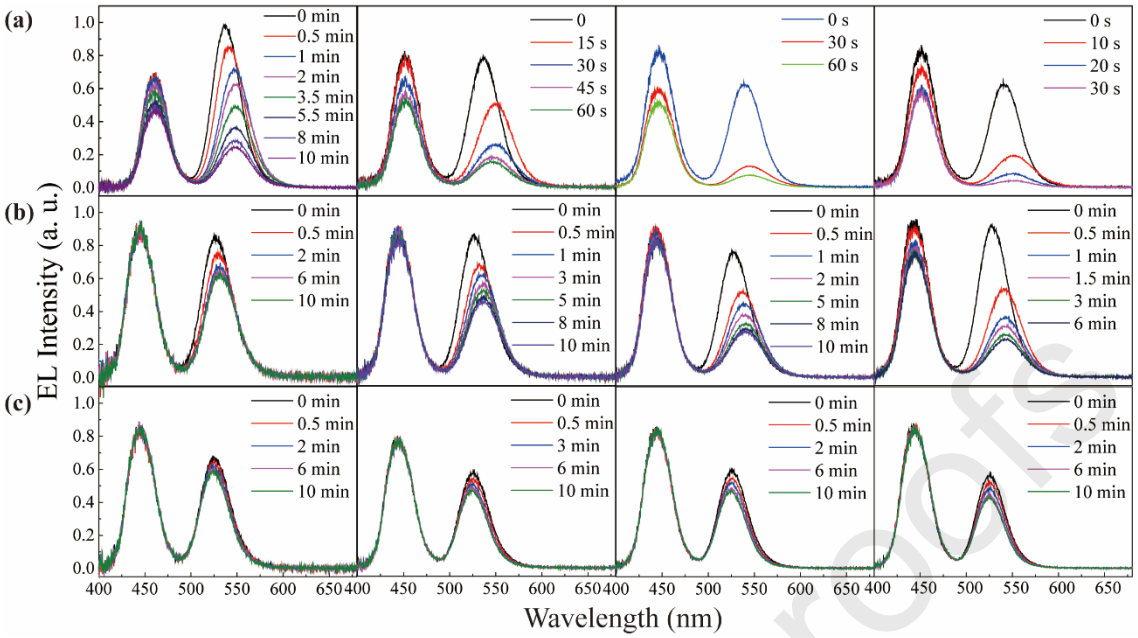

Fig. 9. Electroluminescence (EL) spectra stability of QD-HPLEDs with different injection electrical powers vs. time. (a) On-chip structure; (b) remote structure; (c) wc-remote structure.

The unstable EL spectra also affect the output color of the QD-HPEDs, as well as the EL intensity; their color stabilities represented by the CIE 1931 chromatic coordinates are given in Fig. 10. The color stabilities of the on-chip and remote structures are shown in Figs. 10(a) and (b), respectively, which quickly shift toward the blue region. In particular, the color coordinates of the on-chip structure shift to the blue boundary within 30 s at an injection electrical power of 100 W. Meanwhile, the color shift of the remote structure is not as severe as those discussed above; the wc-remote structure greatly suppresses the color shift, as shown in Fig. 10(c). Interestingly, the color coordinates of the on-chip and remote structures change nonlinearly, while those for the wc-remote structure are almost linear, which can be attributed to the redshift of the green peak in the on-chip and remote structures.

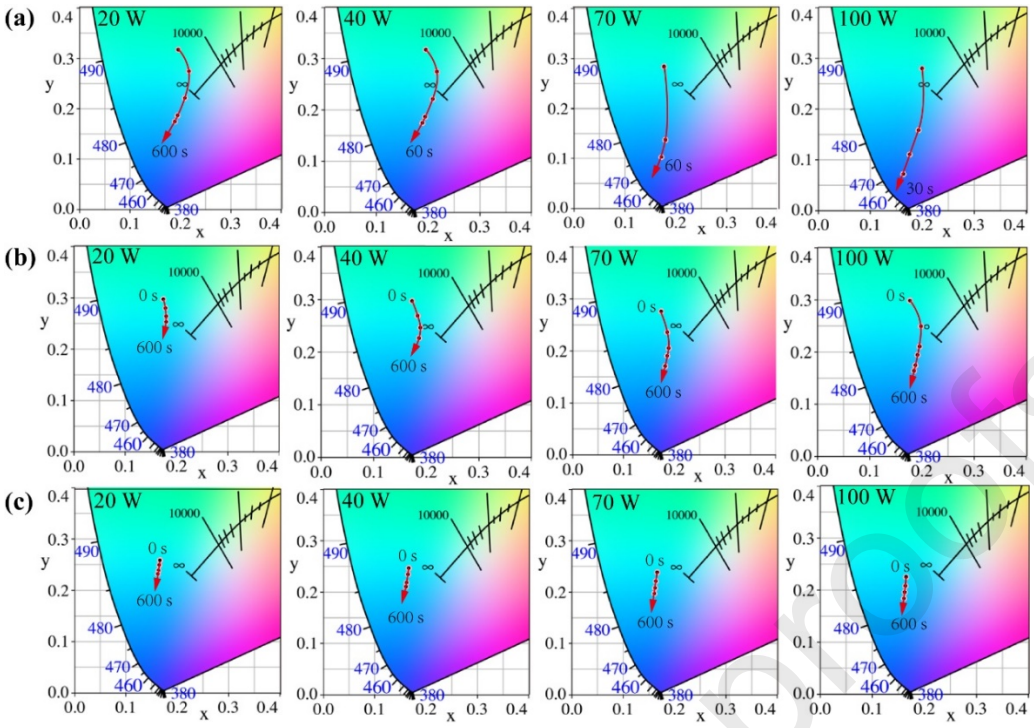

Fig. 10. CIE 1931 chromatic coordinates of QD-HPLEDs with different injection electrical powers vs. operating time. (a) On-chip structure; (b) remote structure; (c) wc-remote structure.

The radiant power and luminous flux stability are significant to ensure the valid operating time of LEDs[46, 47], which are shown in Figs. 11 and 12, respectively. In our cases, we were more concerned about the green peak stability associated with the QD converters. Therefore, the device lifetime is defined as the operating time until the luminous flux of the QD-HPLEDs reduces to 60% of the initial value, which is more sensitive to the green peak. Moreover, the radiant power and luminous flux of the on-chip and remote structures decrease quickly. As discussed above, the fast degradation is attributed to the thermal quenching of QDs and the carbonization of silicone matrixes. Under an injection electrical power of 100 W, the luminous flux of the on-chip structure reduces by 90% in just 60 s, while that of the remote structure reduces by 70% in 6 min, demonstrating that the remote strategy is highly expected by suppression of the heat transfer from the chips to the QDs. As for the wc-remote structure, the luminous flux decreases by only 25% in 10 min owing to the low operating temperature of the QD converter, which is still effective (not reach the lifetime) after operating for 10 min at 100 W of injection electrical power. Therefore, a longer aging test was conducted to measure the lifetime of the wc-remote structure at a typical injection electrical power of 100 W.

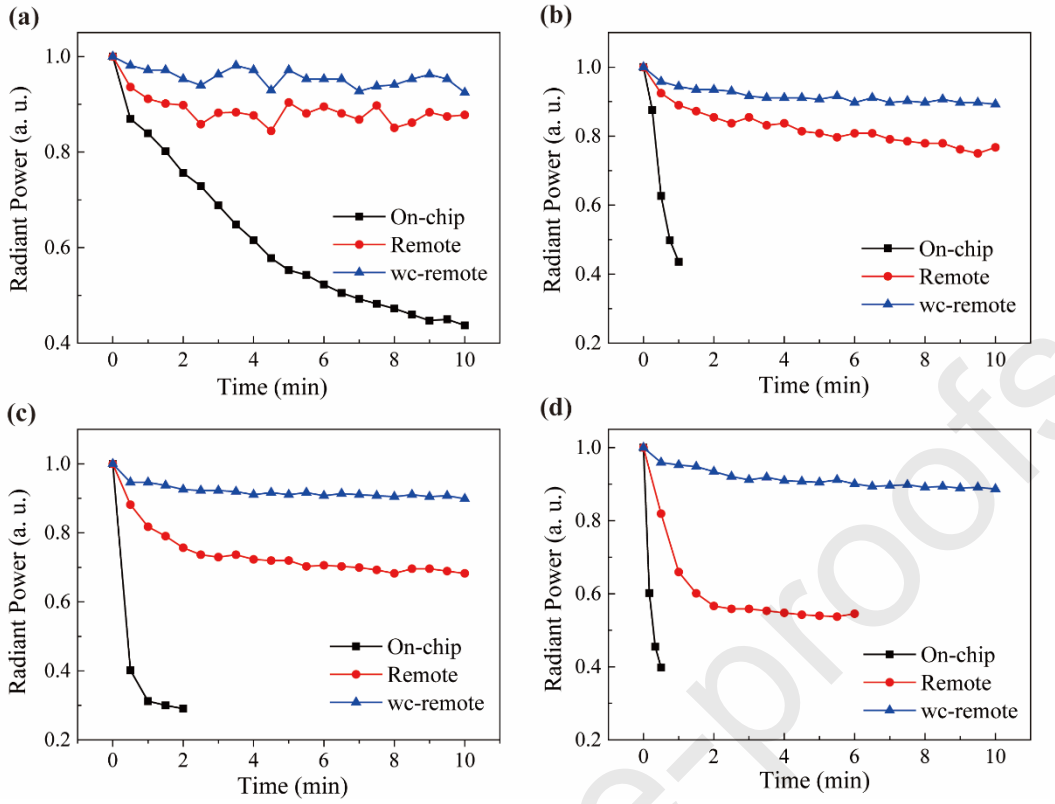

Fig. 11. Radiant power stability of QD-HPLEDs with different injection electrical powers. (a)–(d) Injection electrical power of 20, 40, 70, and 100 W, respectively.

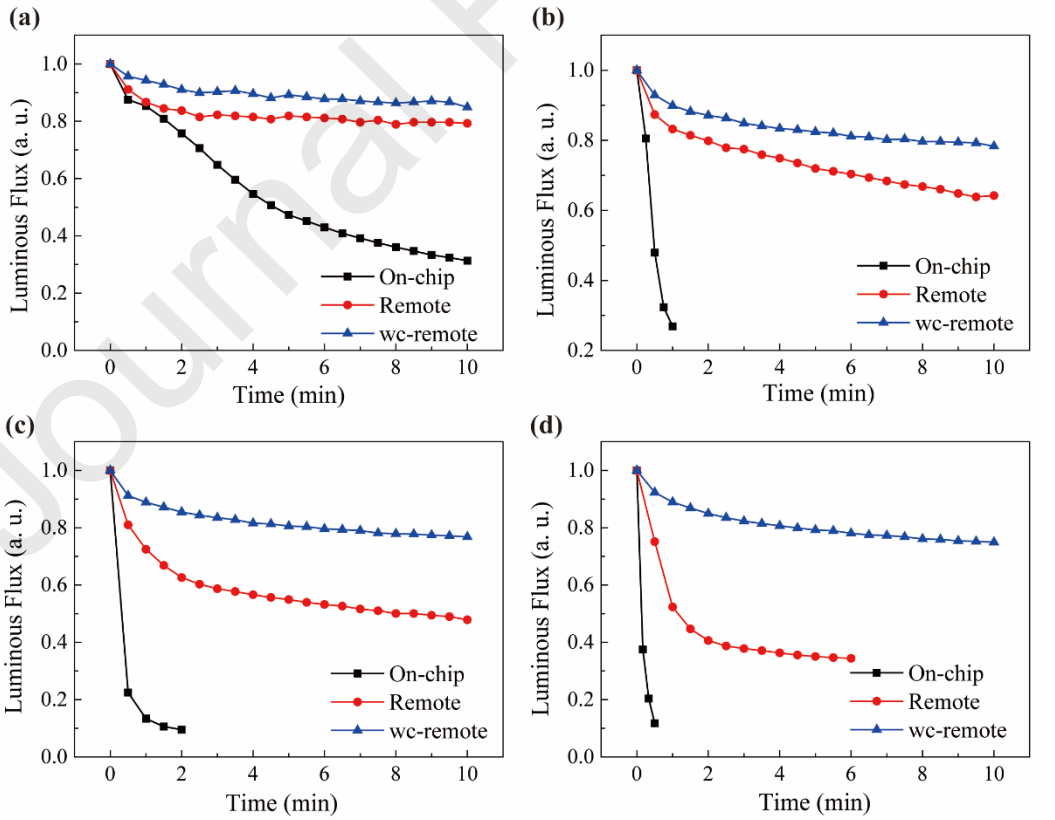

Fig. 12. Luminous flux stability of QD-HPLEDs with different injection electrical powers. (a)–(d)

Injection electrical power of 20, 40, 70, and 100 W, respectively.

The long-time EL spectra stability of the optimized wc-remote structure (120 mL/min) is given in Fig. 13. After 120 min of the aging experiment, the blue peak intensity shows almost no decrement while the green peak intensity decreases by 42.2% from 0 to 120 min. The spectra show almost no redshift and tend to be stable after operating for 70 min. Their radiant power and luminous flux stability are summarized in Fig. 14. The luminous flux and radiant power decrease fast at the initial stage, similar to previous studies, at low working power[22], and tend to increase instability as the operating time increases. Additionally, the lifetime of the on-chip, remote, and optimized wc-remote structures are summarized in the insert. The lifetime of QD-LEDs with the optimized wc-remote structure is 95 min under an optimal flow rate of 120 ml/min, while those of the on-chip structure and remote structures are 6 and 50 s, respectively, showing an increase of 2~3 orders of magnitude. We believe that the device lifetime can be further improved by optimizing the shape parameters of the SGC, the thickness of QDs films, and the packaging material of QDs in order to satisfy the practical applications. Nevertheless, these results confirm that the wc-remote structure contributes to a longer QD-HPLED lifetime, even at an ultrahigh injection electrical power of 100 W. These excellent performances can be a respectable start point for QD converters in one-hundred-watt-level applications, such as projection illumination and display.

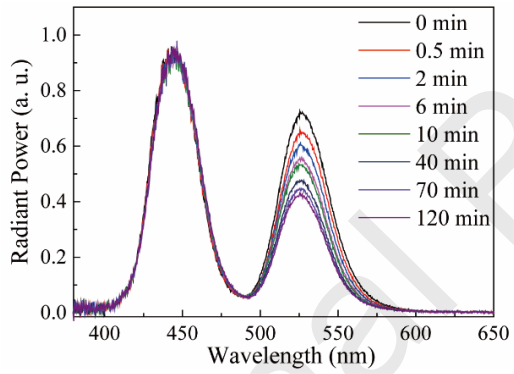

Fig. 13. EL spectra stability of HPLEDs with the optimized wc-remote structure under an injection electrical power of 100 W.

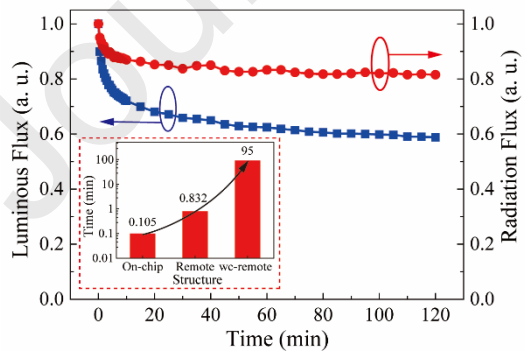

Fig. 14. Luminous flux and radiant power stability of HPLEDs with the wc-remote structure under an injection electrical power of 100 W. The inset summarizes the lifetimes of the QD-HPLEDs with on-chip, remote, and optimized remote structures, respectively, under an injection electrical power of 100 W.

4. Conclusion

In this paper, the wc-remote structure was proposed to improve the heat dissipation and optical stability of QD converters in a HPLED system. We introduced a SGC to improve the heat dissipation of the QD converter, which has almost no effect on the light output, preserving a high optical efficiency. The maximum steady temperature of the wc-remote shows almost no reduction when the flow rate reaches 120 mL/min, which is treated as the optimal flow rate that verified by the fluid and thermal coupling simulation. By comparing the thermal performance and optical stability of the wc-remote structure with the on-chip and remote structures, the excellent heat dissipation and optical stability of the wc-remote structure were demonstrated. Under 100 W of injection electrical power, the maximum steady temperature of the wc-remote structure under an optimized flow rate of 120 mL/min reduced to 71 °C, which reduced by 453 and 265 °C compared with the other structures, respectively. Furthermore, the optical spectra of the wc-remote structure show a slow degradation and almost no redshift, which contributes to lifetime 2~3 orders of magnitude longer than that of conventional structures. Therefore, the wc-remote structure can largely prolong the lifetime from 0.105 min (on-chip structure) and 0.832 min (remote structure) to 95 min. Consequently, the operating temperature and optical stability of QD-HPLEDs can be significantly improved using the wc-remote structure. The wc-remote structure reported herein can be a respectable start point for QD converters in hundred-watt-level applications, such as projection illumination and display.

Acknowledgement

This work was supported by the National Natural Science Foundation of China (No. 51775199 and No. 51735004), the Project of Science and Technology New Star in Zhujiang Guangzhou City (No. 201806010102), and the Natural Science Foundation of Guangdong Province (No. 2018B030306008).

References

[1] E.F. Schubert, J.K. Kim, Solid-state light sources getting smart, Science, 308 (2005) 1274-1278.

[2] F.M. Steranka, J. Bhat, D. Collins, L. Cook, M.G. Craford, R. Fletcher, N. Gardner, P. Grillot, W. Goetz, M. Keuper, R. Khare, A. Kim, M. Krames, G. Harbers, M. Ludowise, P.S. Martin, M. Misra, G. Mueller, R. Mueller-Mach, S. Rudaz, Y.C. Shen, D. Steigerwald, S. Stockman, S. Subramanya, T. Trottier, J.J. Wierer, High Power LEDs - Technology Status and Market Applications, physica status solidi (a), 194 (2002) 380-388.

[3] D.F. Feezell, J.S. Speck, S.P. DenBaars, S. Nakamura, Semipolar InGaN/GaN lightemitting diodes for high-efficiency solid-state, Journal of Display Technology, 9 (2013) 190-198.

[4] H.A. Hoppe, Recent developments in the field of inorganic phosphors, Angew Chem Int Ed Engl, 48 (2009) 3572-3582.

[5] S.H. Lee, D.S. Jung, J.M. Han, H. Young Koo, Y.C. Kang, Fine-sized Y3Al5O12:Ce phosphor powders prepared by spray pyrolysis from the spray solution with barium fluoride flux, Journal of Alloys and Compounds, 477 (2009) 776-779.

[6] G.H. Liu, Z.Z. Zhou, Y. Shi, Q. Liu, J.Q. Wan, Y.B. Pan, Ce:YAG transparent ceramics for applications of high power LEDs: Thickness effects and high temperature performance, Materials Letters, 139 (2015) 480-482.

[7] X. Dai, Z. Zhang, Y. Jin, Y. Niu, H. Cao, X. Liang, L. Chen, J. Wang, X. Peng, Solution-processed, high-performance light-emitting diodes based on quantum dots, Nature, 515 (2014) 96-99.

[8] Y. Shirasaki, G.J. Supran, M.G. Bawendi, V. Bulović, Emergence of colloidal quantum-dot light-emitting technologies, Nature Photonics, 7 (2012) 13-23.

[9] Z. Li, C. Song, J. Li, G. Liang, L. Rao, S. Yu, X. Ding, Y. Tang, B. Yu, J. Ou, U. Lemmer, G. Gomard, Highly Efficient and Water-Stable Lead Halide Perovskite Quantum Dots Using Superhydrophobic Aerogel Inorganic Matrix for White Light-Emitting Diodes, Advanced Materials Technologies, (2020).

[10] E. Jang, S. Jun, H. Jang, J. Lim, B. Kim, Y. Kim, White-light-emitting diodes with quantum dot color converters for display backlights, Adv Mater, 22 (2010) 3076-3080.

[11] B. Xie, R. Hu, X. Luo, Quantum Dots-Converted Light-Emitting Diodes Packaging for Lighting and Display: Status and Perspectives, Journal of Electronic Packaging, 138 (2016).

[12] W. Chen, K. Wang, J.J. Hao, D. Wu, J. Qin, D. Dong, J. Deng, Y.W. Li, Y.L. Chen, W.Q. Cao, High Efficiency and Color Rendering Quantum Dots White Light Emitting Diodes Optimized by Luminescent Microspheres Incorporating, Nanophotonics, 5 (2016) 565-572.

[13] K.T. Shimizu, M. Bohmer, D. Estrada, S. Gangwal, S. Grabowski, H. Bechtel, E. Kang, K.J. Vampola, D. Chamberlin, O.B. Shchekin, J. Bhardwaj, Toward commercial realization of quantum dot based white light-emitting diodes for general illumination, Photonics Research, 5 (2017) A1-A6.

[14] C.-J. Weng, Advanced thermal enhancement and management of LED packages, International Communications in Heat and Mass Transfer, 36 (2009) 245-248.

[15] B. Xie, H.C. Liu, R. Hu, C.F. Wang, J.J. Hao, K. Wang, X.B. Luo, Targeting Cooling for Quantum Dots in White QDs-LEDs by Hexagonal Boron Nitride Platelets with Electrostatic Bonding, Advanced Functional Materials, 28 (2018).

[16] X.R. Ding, M. Li, Z.T. Li, Y. Tang, Y.X. Xie, X.T. Tang, T. Fu, Thermal and optical investigations of a laser-driven phosphor converter coated on a heat pipe, Applied Thermal

Engineering, 148 (2019) 1099-1106.
[17] J.-S. Li, Y. Tang, Z.-T. Li, W.-Q. Kang, X.-R. Ding, B.-H. Yu, Study on Reabsorption Properties of Quantum Dot Color Convertors for Light-Emitting Diode Packaging, Journal of Electronic Packaging, 141 (2019).
[18] B. Xie, R. Hu, X.J. Yu, B.F. Shang, Y.P. Ma, X.B. Luo, Effect of Packaging Method on Performance of Light-Emitting Diodes With Quantum Dot Phosphor, IEEE Photonics Technology Letters, 28 (2016) 1115-1118.
[19] J. Ziegler, S. Xu, E. Kucur, F. Meister, M. Batentschuk, F. Gindele, T. Nann, Silica-Coated InP/ZnS Nanocrystals as Converter Material in White LEDs, Adv Mater, 20 (2008) 4068-4073.
[20] H. Shun-Chieh, C. Yin-Han, T. Zong-Yi, H. Hau-Vei, L. Shih-Li, C. Teng-Ming, K. Hao-Chung, L. Chien-Chung, Highly Stable and Efficient Hybrid Quantum Dot Light-Emitting Diodes, IEEE Photonics Journal, 7 (2015) 1-10.
[21] B. Xie, H. Liu, R. Hu, C. Wang, J. Hao, K. Wang, X. Luo, Targeting Cooling for Quantum Dots in White QDs-LEDs by Hexagonal Boron Nitride Platelets with Electrostatic Bonding, Advanced Functional Materials, 28 (2018).
[22] B. Xie, Y. Cheng, J. Hao, X. Yu, W. Shu, K. Wang, X. Luo, White Light-Emitting Diodes With Enhanced Efficiency and Thermal Stability Optimized by Quantum Dots-Silica Nanoparticles, IEEE Transactions on Electron Devices, 65 (2018) 605-609.
[23] Z.-T. Li, C.-J. Song, Z.-Y. Qiu, J.-S. Li, K. Cao, X.-R. Ding, Y. Tang, Study on the Thermal and Optical Performance of Quantum Dot White Light-Emitting Diodes Using Metal-Based Inverted Packaging Structure, IEEE Transactions on Electron Devices, 66 (2019) 3020-3027.
[24] J.-S. Li, Y. Tang, Z.-T. Li, G.-W. Liang, X.-R. Ding, B.-H. Yu, High Thermal Performance and Reliability of Quantum-Dot-Based Light-Emitting Diodes With Watt-Level Injection Power, IEEE Transactions on Device and Materials Reliability, 19 (2019) 120-125.
[25] Z.-T. Li, J.-X. Li, J.-S. Li, X.-W. Du, C.-J. Song, Y. Tang, Thermal Impact of LED Chips on Quantum Dots in Remote-Chip and On-Chip Packaging Structures, IEEE Transactions on Electron Devices, 66 (2019) 4817-4822.
[26] E. Kim, H.W. Shim, S. Unithrattil, Y.H. Kim, H. Choi, K.J. Ahn, J.S. Kwak, S. Kim, H. Yoon, W.B. Im, Effective Heat Dissipation from Color-Converting Plates in High-Power White Light Emitting Diodes by Transparent Graphene Wrapping, ACS Nano, 10 (2016) 238-245.
[27] Y. Peng, Y. Mou, T. Wang, H. Wang, R. Liang, X. Wang, M. Chen, X. Luo, Effective Heat Dissipation of QD-Based WLEDs by Stacking QD Film on Heat-Conducting Phosphor-Sapphire Composite, IEEE Transactions on Electron Devices, 66 (2019) 2637-2642.
[28] L. Chen, D. Deng, Q. Huang, X. Xu, Y. Xie, Development and thermal performance of a vapor chamber with multi-artery reentrant microchannels for high-power LED, Applied Thermal Engineering, (2019).
[29] X.H. Lin, S.P. Mo, L.S. Jia, Z. Yang, Y. Chen, Z.D. Cheng, Experimental study and Taguchi analysis on LED cooling by thermoelectric cooler integrated with microchannel heat sink, Applied Energy, 242 (2019) 232-238.
[30] D. Sun, G. Liu, L. Shen, H. Chen, Y. Yao, S. Jin, Modeling of high power light-emitting diode package integrated with micro-thermoelectric cooler under various interfacial and size effects, Energy Conversion And Management, 179 (2019) 81-90.
[31] H. Wang, J. Qu, Y.Q. Peng, Q. Sun, Heat transfer performance of a novel tubular oscillating heat pipe with sintered copper particles inside flat-plate evaporator and high-power LED heat sink

application, Energy Conversion And Management, 189 (2019) 215-222.
[32] C. Xiao, H. Liao, Y. Wang, J. Li, W. Zhu, A novel automated heat-pipe cooling device for high-power LEDs, Applied Thermal Engineering, 111 (2017) 1320-1329.
[33] Y.W. Wang, J.W. Cen, F.M. Jiang, W.J. Cao, Heat dissipation of high-power light emitting diode chip on board by a novel flat plate heat pipe, Applied Thermal Engineering, 123 (2017) 19-28.
[34] Z.-T. Li, K. Cao, J.-S. Li, Y. Tang, L. Xu, X.-R. Ding, B.-H. Yu, Investigation of Light-Extraction Mechanisms of Multiscale Patterned Arrays With Rough Morphology for GaN-Based Thin-Film LEDs, IEEE Access, 7 (2019) 73890-73898.
[35] Y. Tang, H.G. Lu, J.S. Li, Z.T. Li, X.W. Du, X.R. Ding, B.H. Yu, Improvement of Optical and Thermal Properties for Quantum Dots WLEDs by Controlling Layer Location, IEEE Access, 7 (2019) 77642-77648.
[36] S.D. Yu, Y. Tang, Z.T. Li, K.H. Chen, X.R. Ding, B.H. Yu, Enhanced optical and thermal performance of white light-emitting diodes with horizontally layered quantum dots phosphor nanocomposites, Photonics Research, 6 (2018) 90-98.
[37] L. Orloff, J. De Ris, G.H. Markstein, Upward turbulent fire spread and burning of fuel surface, Symposium (International) on Combustion, 15 (1975) 183-192.
[38] F. Jiang, J.L. de Ris, M.M. Khan, Absorption of thermal energy in PMMA by in-depth radiation, Fire Safety Journal, 44 (2009) 106-112.
[39] B. Xie, W. Chen, J. Hao, D. Wu, X. Yu, Y. Chen, R. Hu, K. Wang, X. Luo, Structural optimization for remote white light-emitting diodes with quantum dots and phosphor: packaging sequence matters, Opt Express, 24 (2016) A1560-A1570.
[40] X. Luo, X. Fu, F. Chen, H. Zheng, Phosphor self-heating in phosphor converted light emitting diode packaging, International Journal of Heat and Mass Transfer, 58 (2013) 276-281.
[41] K.R. Shailesh, C.P. Kurian, S.G. Kini, Measurement of junction temperature of light-emitting diodes in a luminaire, Lighting Research & Technology, 47 (2014) 620-632.
[42] D. Yang, Y. Xie, C. Geng, C. Shen, J.G. Liu, M. Sun, S. Li, W. Bi, S. Xu, Thermal Analysis and Performance Optimization of Quantum Dots in LEDs by Microsphere Model, IEEE Transactions on Electron Devices, 66 (2019) 3896-3902.
[43] S.V. Garimella, C.B. Sobhan, Transport In Microchannels - a Critical Review, Annual Review of Heat Transfer, 13 (2003) 1-50.
[44] J. Liu, C.L. Xu, H. Zheng, S. Liu, Numerical Analysis and Optimization of Thermal Performance of LED Filament Light Bulb, 2017 Ieee 67th Electronic Components And Technology Conference (Ectc 2017), (2017) 2243-2248.
[45] M.L.V. Ramires, C.A. Nieto de Castro, Y. Nagasaka, A. Nagashima, M.J. Assael, W.A. Wakeham, Standard Reference Data for the Thermal Conductivity of Water, Journal of Physical and Chemical Reference Data, 24 (1995) 1377-1381.
[46] M. Cai, D.G. Yang, J.N. Zheng, Y.Z. Mo, J.L. Huang, J.W. Xu, W.B. Chen, G.Q. Zhang, X.P. Chen, Thermal degradation kinetics of LED lamps in step-up-stress and step-down-stress accelerated degradation testing, Applied Thermal Engineering, 107 (2016) 918-926.
[47] Y. Xie, D. Yang, L. Zhang, Z. Zhang, C. Geng, C. Shen, J.G. Liu, S. Xu, W. Bi, Highly Efficient and Thermal-Stable QD-LEDs Based on Quantum Dots-SiO2-BN Nanoplate Assemblies, ACS Appl Mater Interfaces, (2019).

Highlights

- A wc-remote structure is introduced to high power LED systems.
- The temperature of QD converters is reduced by 383℃ at 100 W injection power.
- The device lifetime is increased by orders of magnitude at 100 W injection power.